Ni- and Ni/Pd-Catalyzed Reductive Coupling of Lignin-Derived Aromatics to Access Biobased Plasticizers

Zhi-Ming Su, Jack Twilton, Caroline B. Hoyt, Fei Wang, Lisa Stanley, Heather B. Mayes, Kai Kang, Daniel J. Weix, Gregg T. Beckham,* and Shannon S. Stahl*

ACCESS | Metrics & More | Article Recommendations | SI Supporting Information

ABSTRACT: Lignin-derived aromatic chemicals offer a compelling alternative to petrochemical feedstocks, and new applications are the focus of extensive interest. 4-Hydroxybenzoic acid (**H**), vanillic acid (**G**), and syringic acid (**S**) are readily obtained via oxidative depolymerization of hardwood lignin substrates. Here, we explore the use of these compounds to access biaryl dicarboxylate esters that represent biobased, less toxic alternatives to phthalate plasticizers. Chemical and electrochemical methods are developed for catalytic reductive coupling of sulfonate derivatives of **H**, **G**, and **S** to access all possible homo- and cross-coupling products. A conventional NiCl$_2$/bipyridine catalyst is able to access the **H**−**H** and **G**−**G** products, but new catalysts are identified to afford the more challenging coupling products, including a NiCl$_2$/bisphosphine catalyst for **S**−**S** and a NiCl$_2$/phenanthroline/PdCl$_2$/phosphine cocatalyst system for **H**−**G**, **H**−**S**, and **G**−**S**. High-throughput experimentation methods with a chemical reductant (Zn powder) are shown to provide an efficient screening platform for identification of new catalysts, while electrochemical methods can access improved yields and/or facilitate implementation on larger scale. Plasticizer tests are performed with poly(vinyl chloride), using esters of the 4,4′-biaryl dicarboxylate products. The **H**−**G** and **G**−**G** derivatives, in particular, exhibit performance advantages relative to an established petroleum-based phthalate ester plasticizer.
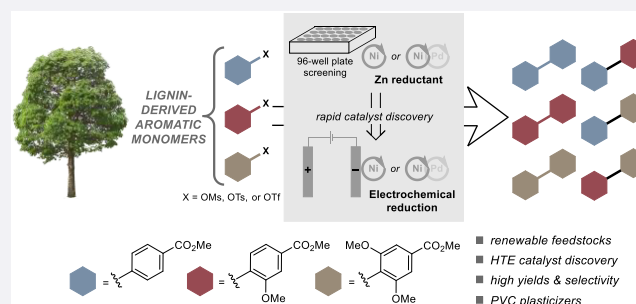
INTRODUCTION

Lignin represents the largest source of biomass-derived aromatic chemicals and is an ideal supplement or alternative to petroleum-based feedstocks.[1−9] Significant progress has been made in lignin depolymerization into aromatic monomers,[4−9] but methods for conversion of lignin-derived monomers (LDMs) into value-added chemicals are still in the nascent stages of development.[1−3,10] In connection with efforts focused on oxidative lignin depolymerization,[11−13] we recognized that some of the most common products, 4-hydroxybenzoic acid (**H**), vanillic acid (**G**), and syringic acid (**S**), could serve as precursors to biaryl dicarboxylates (Figure 1).[14] The parent analogue, biphenyl-4,4′-dicarboxylic acid (BPDA), has been the focus of commercial interest as a monomer for polyesters and as the core structure for nonphthalate plasticizers for poly(vinyl chloride) (PVC).[15−18] Existing methods for the synthesis of BPDA use petroleum-based precursors in multistep routes (e.g., involving oxidative coupling, alkylation, and/or dehydrogenation steps, paired with autoxidation of alkyl groups into carboxylic acids), and they often afford a mixture of regioisomers.[16,19−21] Reductive coupling of phenol derivatives represents a different route to BPDA derivatives that accesses a single product regioisomer. The biomass-derived **H** compound provides a
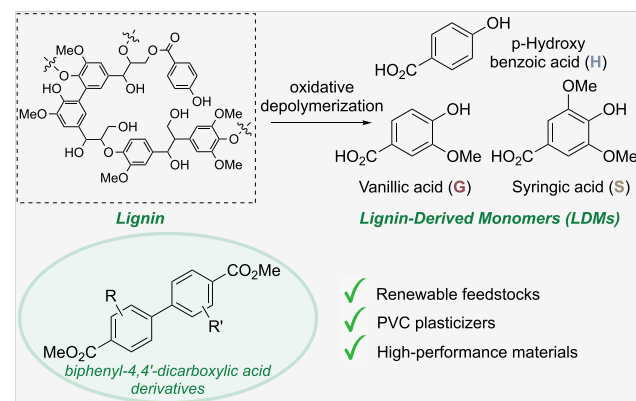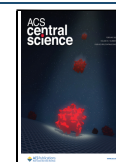
Figure 1. Lignin is an abundant biomass-derived source of aromatics that represent potential precursors to commercially important biphenyl-4,4′-dicarboxylates.

means to access the same BPDA analogue currently sourced from petroleum, while the **G** and **S** compounds that have methoxy substituents will afford BPDA derivatives that could have favorable properties (e.g., as a PVC plasticizer).
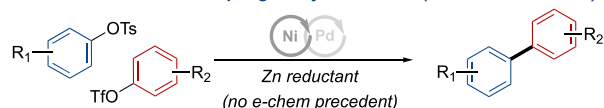
We postulated that the **H**, **G**, and **S** products of lignin depolymerization could be readily converted to aryl sulfonates amenable to reductive cross-coupling. Ni-catalyzed coupling of aryl electrophiles to access biaryls was first reported in the 1970s, and the field advanced significantly in subsequent decades.[22−31] These reactions typically feature stoichiometric metal reductants, such as Zn powder, but important electrochemical precedents also exist. Several examples provide an important foundation for the present work. In 1995, Percec et al. demonstrated that a Ni/PPh₃ catalyst system with Zn reductant promotes homocoupling of aryl sulfonates to biaryls (Scheme 1A).[32] Shortly thereafter, Jutand and co-workers

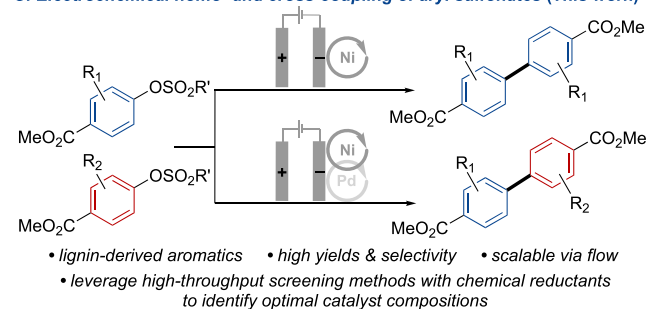## Scheme 1. Precedents Relevant to Reductive Coupling of Lignin-Derived Aryl Sulfonates

A: Homocoupling of aryl sulfonates (Percec, Jutand)
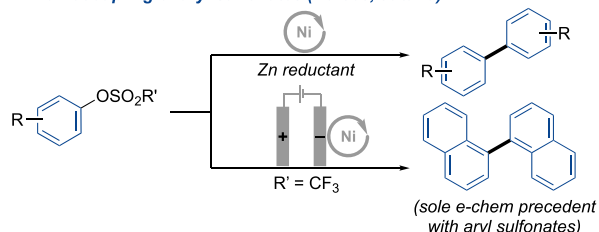
B: Zn-mediated cross-coupling of aryl sulfonates (Weix & Kramer/Lian)

C: Electrochemical homo- and cross-coupling of aryl sulfonates (This work)

• lignin-derived aromatics   • high yields & selectivity   • scalable via flow
• leverage high-throughput screening methods with chemical reductants to identify optimal catalyst compositions

achieved homocoupling of aryl triflates with phosphine-ligated Pd *or* Ni catalysts. This study included a single example of electrochemical Ni-catalyzed homocoupling, using 1-naphthyl triflate as the substrate (Scheme 1A).[29,30,33] In recent years, Weix and co-workers have developed methods for selective cross-coupling of aryl electrophiles with a cocatalyst system containing both Ni and Pd in the presence of Zn as the reductant.[34−37] The groups of Weix[37] and Kramer/Lian[38] independently reported reductive cross-coupling of two different aryl sulfonates by pairing Pd/bisphosphine and Ni/diimine cocatalysts [diimine = substituted 2,2′-bipyridine (bpy) or 1,10-phenanthroline (phen) derivatives] with Zn (Scheme 1B). To date, no electrochemical methods to our knowledge have been reported for reductive cross-coupling of phenol derivatives (Scheme 1C).[39−42]

Chemical and electrochemical conditions have complementary advantages for reductive coupling reactions. Chemical

conditions are more straightforward to implement on small scale, owing to their use of standard laboratory equipment, and they are more amenable to high-throughput experimentation (HTE) techniques for catalyst discovery and reaction optimization. Electrochemical methods offer advantages for large scale applications by avoiding the challenges of handling dense metal-powder reagents and creating opportunities to improve sustainability. Although advances have been made in the development of electrochemical reactors for parallel reaction screening,[43,44] chemical HTE methodology retains substantially improved efficiency and is compatible with smaller quantities of reagents. In this context, we postulated that HTE screening methods using chemical reductants could enable rapid identification of promising catalyst systems and conditions for subsequent development of electrochemical methods. The results outlined below validate this hypothesis and achieve successful chemical and electrochemical conditions for all possible homo- and cross-coupling permutations between **H**-, **G**-, and **S**-derived reaction partners. Additional important outcomes of this study include (a) identification of mono- and bidentate phosphine ligands that lack precedent in Ni-catalyzed reductive coupling reactions, (b) successful adaptation of catalysts from chemical to electrochemical conditions, with matching or superior performance, (c) the first demonstration of Ni/Pd cocatalyzed reductive biaryl cross-coupling under electrochemical conditions, and (d) data showing that biaryl dicarboxylic esters prepared from LDMs exhibit improved PVC plasticizer performance and reduced toxicity relative to a commercial phthalate-based plasticizer.[45]

■ RESULTS AND DISCUSSION

Ni-Catalyzed Homocoupling of LDMs. The methyl esters of **H**, **G**, and **S** are readily converted into electrophiles by reaction of the phenols with sulfonyl chlorides, RSO₂Cl [R = methyl (Ms) or tosyl (Ts)], or triflic anhydride (Tf₂O). Initial studies evaluated the electrochemical homocoupling of methyl 3-methoxy-4-((methylsulfonyl)oxy)benzoate (**G−OMs**). The two possible byproducts are denoted as the Ar−H and ArO−H species, derived from reductive cleavage of the C−O or the S−O bond of the **G−OMs** substrate. A combination of NiCl₂(dme)/bpy has been used previously for reductive homocoupling of Ar−X species[29,30] and this catalyst system was tested initially in an undivided cell with LiBr as the electrolyte and stainless steel as the anode. However, these conditions only afforded the **G−G** product in 29% yield, with a significant amount of byproduct and unreacted starting material (Table 1, entry 1). Use of increased bpy ligand loading (bpy:Ni = 3:1) stabilizes the catalyst[46] and leads to a higher yield of the desired product (72%), together with the Ar−H byproduct (27%; Table 1, entry 2). Other sacrificial anodes were tested in an effort to optimize the yield of biaryl product (Table 1, entries 3−5). Significant reductive C−O cleavage was also observed when Al or Zn was used as the anode (Table 1, entries 3 and 4). This C−O cleavage is rationalized by previous observations that aryl-Ni species can transfer an aryl group to Zn²⁺, generating aryl-Zn species that are susceptible to protonolysis and Ar−H byproduct formation.[37,47] Electrolysis in an undivided cell using a Mg anode proved ineffective (Table 1, entry 5). In this case, reductive S−O bond cleavage was favored, likely reflecting single-electron reduction of the sulfonyl group at the Mg surface.[33] These considerations prompted us to test a sacrificial anode with a divided cell configuration that would avoid the

Table 1. Optimization of Electrochemical Ni-Catalyzed Reductive Homocoupling[a]

Entry	Ar–X	Cell type	Anode	Ar–H (%)	ArO–H (%)	Yield (%)
1[b]		undivided	stainless-steel	42	0	29
2		undivided	stainless-steel	27	0	72
3	**G–OMs**	undivided	Al	20	0	20
4		undivided	Zn	95	2	3
5		undivided	Mg	7	37	4
6		divided	stainless-steel	7	4	80
7		**divided**	**Mg**	8	0	**92 (90)**
8[c]	**H–OMs**	divided	Mg	0	0	**99 (97)**
9[c]		undivided	stainless-steel	10	0	89
10	**S–OMs**	divided	Mg	2	1	3

[a]See the Supporting Information for full experimental details. Yields are determined by ^{1}H NMR analysis of the crude reaction mixture using mesitylene as an internal standard; yields shown in parentheses are isolated. [b]5 mol % bpy. The rest of the mass corresponds to unreacted starting material. [c]1 mol % Ni catalyst.

A: Ni-Catalyzed Homocoupling of S–OTf with Zn Reductant[a]

Entry	Ligand	Conversion (%)	Ar–H (%)	ArO–H (%)	Yield (%)
1	bpy	75	26	32	8
2	phen	74	29	34	6
3	4,4'-dPhbpy	82	30	35	10
4	^{t}Butpy	100	38	40	0
5	DPEPhos	82	54	11	16
6	XantPhos	62	33	18	0
7[b]	DPEPhos	98	37	8	38
8[b,c]	**DPEPhos**	100	32	5	**55**

B: Electrochemical Ni-Catalyzed Homocoupling of S–OTf

Figure 2. Ni-catalyzed reductive homocoupling of **S–OTf**: translating conditions optimized with Zn reductant (A) to electrochemical conditions (B). See the Supporting Information for full experimental details. (a) Yields are determined by ^{1}H NMR analysis of the crude reaction mixture using mesitylene as an internal standard; yields shown in parentheses are isolated. (b) 60 °C. (c) DMSO solvent.

contact of substrate with the anode surface and minimize the presence of Lewis acidic metal ions in the cathodic chamber. This hypothesis was validated by observation of a 92% **G–G** product yield when using a Mg anode in a divided cell (Table 1, entry 7). This outcome is noteworthy because it is significantly better than that achieved when performing the same reaction under previously reported chemical conditions[32] or optimized variations thereof with Zn powder as the reductant (48% and 59% **G–G** yields, respectively; Table S1). Use of analogous conditions with **H–OMs** as the substrate leads to near-quantitative yield of the biaryl **H–H** product (Table 1, entry 8). This outcome was achieved, even when lowering the Ni catalyst loading to 1 mol %. Use of a stainless-steel anode in an undivided cell retained good yield (Table 1, entry 9). The latter conditions are readily implemented in a recirculating flow electrolysis cell with a parallel-plate reactor. This approach was used to conduct a larger scale reaction (11 g, 48 mmol **H–OMs**), accessing the **H–H** product in 80% yield with 2 mol % Ni catalyst (see Section 4 of the Supporting Information for details).

The catalyst and conditions identified for homocoupling of **H–OMs** and **G–OMs** proved ineffective with the more sterically demanding syringic acid derivative **S–OMs**. Only trace quantities of **S–S** product were obtained (Table 1, entry 10). To facilitate evaluation of modified conditions, we used a 24-well screening platform with Zn powder as a chemical reductant. The triflate derivative **S–OTf** was found to be more reactive than the mesylate (Table S2), and this substrate was tested with dozens of nitrogen- and phosphine-based ligands. Selected results are summarized in Figure 2A, with full screening data provided in the Supporting Information (see
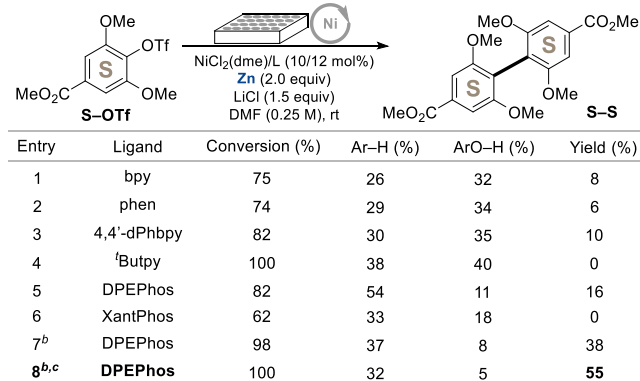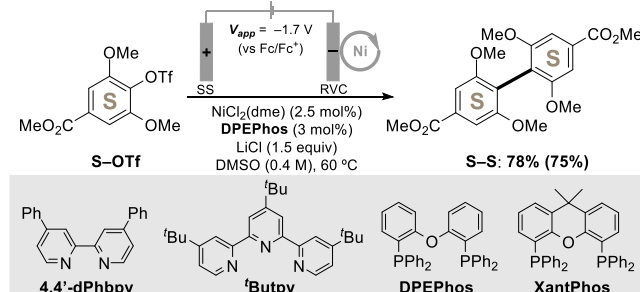
Tables S2–S8). DPEPhos was the only ligand that showed modest success; even the closely related, conformationally more rigid XantPhos ligand was completely ineffective (Figure 2A, entries 5 and 6). Increasing the temperature to 60 °C led to an increase in conversion and product yield (Figure 2A, entry 7), and changing the solvent to DMSO led to a 55% yield of **S–S** (Figure 2A, entry 8). The outcome improved even further when the conditions were adapted to an undivided electrochemical cell with a stainless-steel anode: the desired dimer **S–S** was generated in 78% yield (Figure 2B; see Table S9 for full screening data). This improved electrochemical outcome was achieved, even though the NiCl$_2$/DPEPhos catalyst loading was lowered to 2.5 mol %.

Optimization of Ni/Pd-Catalyzed Cross-Coupling. The Ni-only catalyst systems noted above were evaluated in the cross-coupling of **H**, **G**, and **S** sulfonates; however, these reactions led to poor selectivity and yields of the desired products (Table S10). These complications prompted us to evaluate the recently disclosed dual Ni/Pd cocatalyst systems.[34−38] For example, the method of Weix and co-workers, which employs Ni/Pd chloride salts in combination with 4,4′-diphenyl-bpy (4,4′-dPhbpy) and 1,4-bis-(diphenylphosphino)butane (dppb) and Zn as a chemical reductant, supports cross-coupling of aryl triflates and tosylates.[37] Efforts to translate this catalyst system to electrochemical cross-coupling of **G** and **S** sulfonates were unsuccessful, regardless of the sulfonate activating groups: biaryl products formed in ≤15% yield and favored the homocoupling products (Figure S5). Consequently, we again elected to use the high-throughput experimentation platform
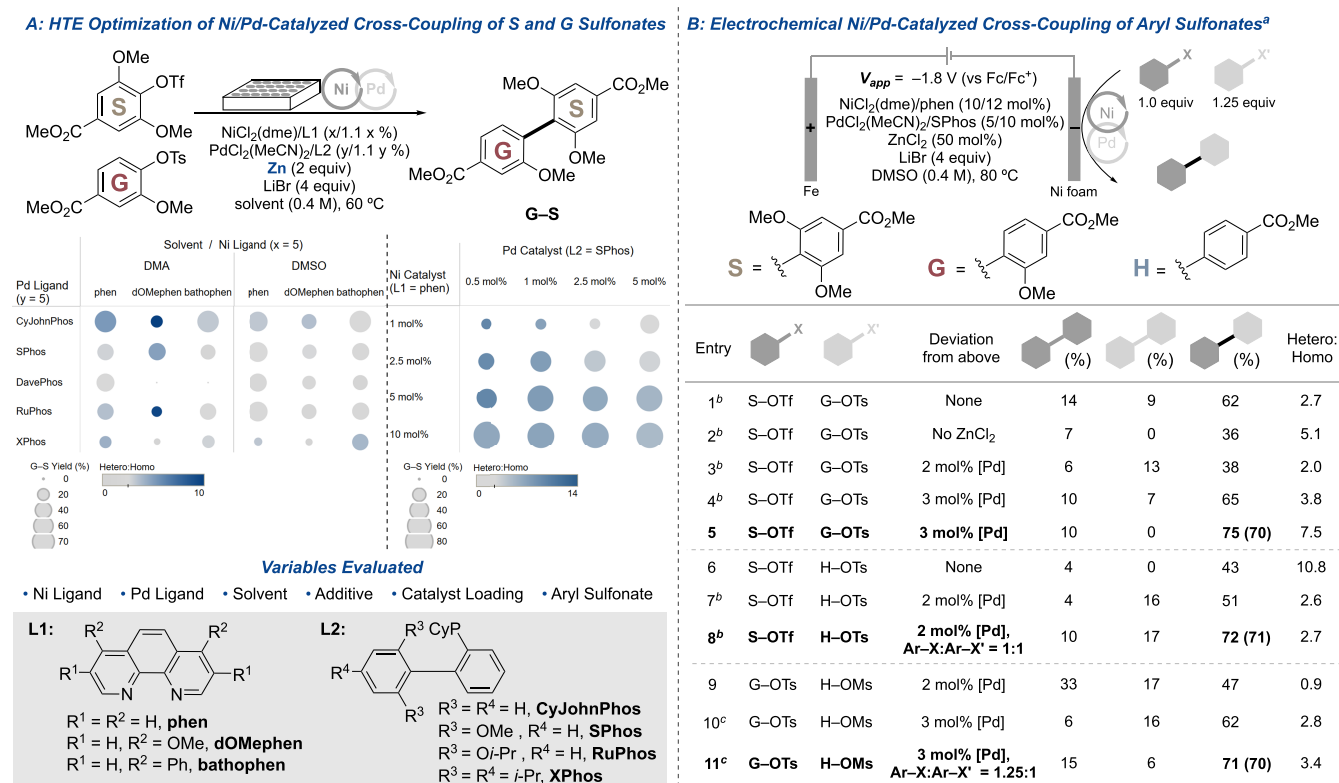
A: HTE Optimization of Ni/Pd-Catalyzed Cross-Coupling of S and G Sulfonates

B: Electrochemical Ni/Pd-Catalyzed Cross-Coupling of Aryl Sulfonates[a]

Entry	X	X'	Deviation from above	(%)	(%)	(%)	Hetero: Homo
1[b]	S–OTf	G–OTs	None	14	9	62	2.7
2[b]	S–OTf	G–OTs	No ZnCl$_2$	7	0	36	5.1
3[b]	S–OTf	G–OTs	2 mol% [Pd]	6	13	38	2.0
4[b]	S–OTf	G–OTs	3 mol% [Pd]	10	7	65	3.8
5	**S–OTf**	**G–OTs**	**3 mol% [Pd]**	**10**	**0**	**75 (70)**	**7.5**
6	S–OTf	H–OTs	None	4	0	43	10.8
7[b]	S–OTf	H–OTs	2 mol% [Pd]	4	16	51	2.6
8[b]	S–OTf	H–OTs	2 mol% [Pd], Ar–X:Ar–X' = 1:1	10	17	**72 (71)**	2.7
9	G–OTs	H–OMs	2 mol% [Pd]	33	17	47	0.9
10[c]	G–OTs	H–OMs	3 mol% [Pd]	6	16	62	2.8
11[c]	**G–OTs**	**H–OMs**	**3 mol% [Pd], Ar–X:Ar–X' = 1.25:1**	15	6	**71 (70)**	3.4

Figure 3. Ni/Pd-catalyzed reductive cross-coupling of lignin-derived aryl sulfonates. (A) HTE optimization of G/S cross-coupling. Left chart: S–OTf:G–OTs = 1:1; right chart: DMSO solvent, S–OTf:G–OTs = 1:1.25. The hetero:homo coupling ratio is defined as **G–S** yield/(**G–G** yield + **S–S** yield). (B) Optimization of electrochemical Ni/Pd-catalyzed cross-coupling. See the Supporting Information for full experimental details. (a) Yields determined by UPLC-MS analysis using 1,3,5-trimethoxybenzene as an internal standard; yields shown in parentheses are isolated. (b) RVC cathode. (c) L1 = 4,4′-dPhbpy, L2 = dppb (3.6 mol %), DMA instead of DMSO, 60 °C.

with Zn as the chemical reductant to evaluate modified conditions. Initial studies focused on cross-coupling of **G** and **S** sulfonates, evaluating different combinations of ligands, solvents, additives, sulfonate activating groups, and Ni/Pd ratios, and the results are visualized in Figure 3A (see Tables S11−S14 for full screening). The size of the circles in these charts corresponds to the yield, while the color reflects the hetero:homo coupling ratio (darker blue reflects higher selectivity). Among the most noteworthy outcome from these experiments is the beneficial effect of bulky biaryl dialkyl monophosphine ligands ("Buchwald ligands"[48]). The utility of these ligands could reflect their ability to promote the difficult reductive elimination steps.[48] CyJohnPhos was the most effective ligand under screening conditions with Zn powder as the reductant (Figure 3A). Subsequent studies revealed that CyJohnPhos decomposes under electrochemical reaction conditions. In contrast, SPhos is stable and supports good reactivity. Further chemical screening evaluated different Ni:Pd ratios in a cocatalyst system derived from NiCl$_2$(dme)/phen and PdCl$_2$(MeCN)$_2$/SPhos (Figure 3A). These studies showed that the highest yields were obtained with 10 mol % Ni and a Pd loading ranging from 0.5 to 5 mol %.

We then initiated electrochemical studies to access cross-coupled products **G−S**, **H−S**, and **H−G**, starting with a cocatalyst composed of 10 mol % NiCl$_2$(dme)/phen and 5 mol % PdCl$_2$(MeCN)$_2$/SPhos (Figure 3B). Promising performance was identified with a reticulated vitreous carbon (RVC) cathode, sacrificial iron anode, and a constant applied potential of −1.8 V vs Fc/Fc⁺. Inclusion of 0.5 equiv of ZnCl$_2$

significantly improved the reaction outcome (Figure 3B, entries 1 and 2), consistent with previous evidence that Zn²⁺ salts mediate transmetalation between Ni and Pd centers.[37,49,50] Increasing the phosphine ligand loading from 1.1 to 2 equiv with respect to Pd stabilized the Pd catalyst. These initial conditions afforded the desired product **G−S** in 62% yield with 23% homocoupled byproducts, similar to the yields obtained in the chemical screening studies with Zn as a chemical reductant. It is not surprising that the reaction selectivity varies somewhat between chemical and electrochemical conditions. One important factor is that the cathode potential will not directly match the reduction potential of Zn, and variations in substrate consumption (i.e., via byproduct formation) will lead to differences in the selectivity between chemical and electrochemical conditions. Also, because the selectivity is dictated by pairing of the Ni and Pd catalytic cycles, different rates of catalyst turnover at the Zn surface (chemical) vs cathode surface (electrochemical) will affect the hetero:homo coupling selectivity. Adjusting the Ni:Pd ratio from 2:1 to 3.3:1 and using a Ni foam cathode instead of RVC increased the **G−S** product yield to 75% (Figure 3B, entries 3−5). Slight modification of these conditions accessed the **H−S** cross-coupling product in 72% yield (Figure 3B, entry 8). Analogous conditions were less effective for cross-coupling of the less sterically demanding **H** and **G** sulfonates (Figure 3B, entry 9), but adaptation of the chemical catalyst system reported by Weix and co-workers proved effective for the cross-coupling of **H−OMs**/**G−OTs**, accessing **H−G** in 71% yield (Figure 3B, entry 11). This reaction represents the first

selective cross-coupling (under chemical or electrochemical conditions) of aryl mesylate/aryl tosylate partners, which are significantly more economical than aryl triflates.

Plasticizer Properties of Lignin-Derived Biaryls. The above results provide access to all possible homo- and cross-coupled BPDA derivatives of **H**, **G**, and **S**. These structures provide the basis for testing of these materials as plasticizers for PVC and comparison of their performance relative to the existing petroleum-derived incumbent, di(2-ethylhexyl)-phthalate (DEHP). Each of the BPDA methyl esters was subjected to Ti(OBu)$_4$-promoted transesterification with 2-ethylhexanol to afford the corresponding DEH−BPDA derivatives, designated **H−H**[PL], **H−G**[PL], **H−S**[PL], **G−G**[PL], **G−S**[PL], and **S−S**[PL]. The thermal properties of these structures were characterized by thermogravimetric analysis (TGA) and differential scanning calorimetry (DSC) (Figure S9, Table S15). DEHP and the DEH−BPDA derivatives were then individually integrated with PVC at 10 wt %, and the materials were analyzed by TGA and DSC to measure their glass transition temperature (T_g) and the temperature at which the polymer degrades with 10% or 50% loss of its original weight (T_{d10}, T_{d50}) (Figures S10 and S11, Table S16). The former metric reflects the ability of the plasticizer to soften PVC, while the latter metrics reflect the thermostability of the plasticized material. Preferred plasticizers will achieve lower T_g and higher T_{d10}/T_{d50} values. The results, summarized in Figure 4, show
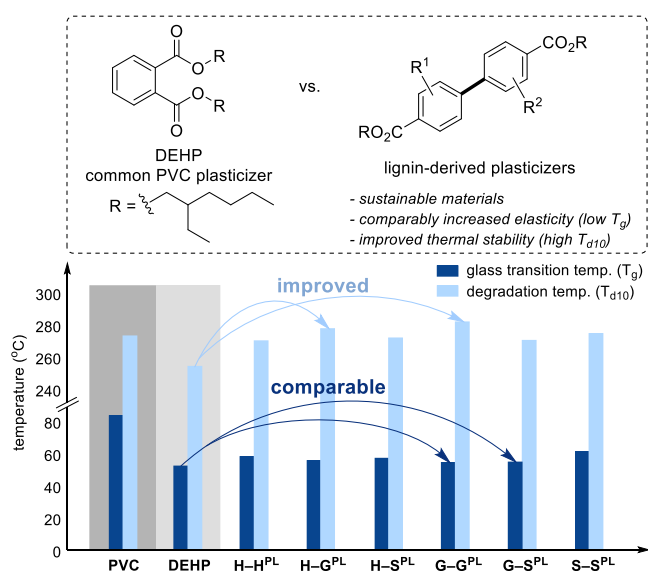

Figure 4. Thermal analysis of lignin-derived biaryl plasticizers. From left to right: unplasticized PVC, 10 wt % plasticized PVC with DEHP, and 10 wt % plasticized PVC with lignin-derived biaryl plasticizers.

that the different plasticizers lower the T_g of PVC from 83.0 to 52.1−61.0 °C. The greatest effect is observed with DEHP, **G−G**[PL], and **G−S**[PL], which lead to T_g values of 52.1, 54.4, and 54.6 °C, respectively. Meanwhile, **H−G**[PL] and **G−G**[PL] show a notable enhancement in thermostability, with these plasticized materials exhibiting even higher T_{d10} (278 and 281 °C) than PVC itself (272 °C), and both outperform DEHP (T_{d10} = 253 °C).

The same series of compounds were then evaluated using tools developed by the US Environmental Protection Agency to predict their potential toxicity[51] and their metabolic and environmental transformation[52] (see Section 7 of the

Supporting Information for details). The results assign these materials to the lowest hazard category with respect to acute toxicity to mammals (>5,000 mg/kg), and the lignin-derived BPDAs arising from hydrolysis of the esters are predicted to be metabolized more easily than phthalic acid. Further experimental studies will be needed to validate this assessment, but these results and the promising performance characteristics in Figure 4 reinforce the potential performance-advantaged properties of biobased plasticizers derived from these BPDAs.

◼ CONCLUSION

The results above demonstrate the utility of Ni- and Ni/Pd-catalyzed cross-electrophile coupling to convert lignin-derived aromatic compounds into a collective of substituted biphenyl dicarboxylic acids. All possible combinations of **H**, **G**, and **S** monomers have been prepared, with symmetrical dimers accessed using a Ni-only catalyst system and the unsymmetrical dimers accessed using Ni/Pd cocatalyst systems. The results highlight the synergy between chemical and electrochemical reduction methods. HTE screening methods with a chemical reductant offer advantages for identification of effective catalyst compositions. For example, chemical HTE methods identified Ni/DPEPhos catalyst and Ni/phen/Pd/SPhos cocatalyst systems, which lacked precedent for homo- and cross-biaryl coupling, respectively. In each case, the chemical reaction conditions were successfully translated to electrochemical conditions, often resulting in improved performance. The beneficial effect of bulky phosphine ligands with the **S**-derived monomers has important implications for other cross-electrophile coupling reactions with sterically congested aryl electrophiles, beyond those studied here. Finally, the new BPDA derivatives bearing methoxy substituents, which are intrinsic to lignin-based aromatics, exhibit appealing plasticizer properties that merit further investigation and development.

◼ ASSOCIATED CONTENT

ⓈI Supporting Information

The Supporting Information is available free of charge at https://pubs.acs.org/doi/10.1021/acscentsci.2c01324.

Complete experimental procedures and compound characterization (PDF)

◼ AUTHOR INFORMATION

Corresponding Authors

Gregg T. Beckham − *Renewable Resources and Enabling Sciences Center, National Renewable Energy Laboratory, Golden, Colorado 80401, United States;* ⓘ orcid.org/0000-0002-3480-212X; Email: gregg.beckham@nrel.gov

Shannon S. Stahl − *Department of Chemistry, University of Wisconsin−Madison, Madison, Wisconsin 53706, United States;* ⓘ orcid.org/0000-0002-9000-7665; Email: stahl@chem.wisc.edu

Authors

Zhi-Ming Su − *Department of Chemistry, University of Wisconsin−Madison, Madison, Wisconsin 53706, United States;* ⓘ orcid.org/0000-0002-1151-0589

Jack Twilton − *Department of Chemistry, University of Wisconsin−Madison, Madison, Wisconsin 53706, United States;* ⓘ orcid.org/0000-0003-3500-4901

Caroline B. Hoyt − *Renewable Resources and Enabling Sciences Center, National Renewable Energy Laboratory, Golden, Colorado 80401, United States*

Fei Wang − *Department of Chemistry, University of Wisconsin−Madison, Madison, Wisconsin 53706, United States;* ● orcid.org/0000-0001-6945-4287

Lisa Stanley − *Renewable Resources and Enabling Sciences Center, National Renewable Energy Laboratory, Golden, Colorado 80401, United States*

Heather B. Mayes − *Renewable Resources and Enabling Sciences Center, National Renewable Energy Laboratory, Golden, Colorado 80401, United States;* ● orcid.org/0000-0001-9373-0106

Kai Kang − *Department of Chemistry, University of Wisconsin−Madison, Madison, Wisconsin 53706, United States;* ● orcid.org/0000-0002-7625-1661

Daniel J. Weix − *Department of Chemistry, University of Wisconsin−Madison, Madison, Wisconsin 53706, United States*

Complete contact information is available at:
https://pubs.acs.org/10.1021/acscentsci.2c01324

Author Contributions

All authors have given approval to the final version of the manuscript.

Notes

The authors declare the following competing financial interest(s): Patent applications have been filed on the electrochemical process and the plasticizers described herein.

◼ REFERENCES

(1) Upton, B. M.; Kasko, A. M. Strategies for the Conversion of Lignin to High-Value Polymeric Materials: Review and Perspective. *Chem. Rev.* **2016**, *116*, 2275−2306.

(2) Fache, M.; Darroman, E.; Besse, V.; Auvergne, R.; Caillol, S.; Boutevin, B. Vanillin, a Promising Biobased Building-Block for Monomer Synthesis. *Green Chem.* **2014**, *16*, 1987−1998.

(3) Gandini, A.; Belgacem, M. N.; Guo, Z.-X.; Montanari, S. Lignins as Macromonomers for Polyesters and Polyurethanes. In *Chemical Modification, Properties and Usage of Lignin*; Hu, T. Q., Ed.; Kluwer Academic/Plenum: New York, 2002; pp 57−80.

(4) Li, C.; Zhao, X.; Wang, A.; Huber, G. W.; Zhang, T. Catalytic Transformation of Lignin for the Production of Chemicals and Fuels. *Chem. Rev.* **2015**, *115*, 11559−11624.

(5) Rinaldi, R.; Jastrzebski, R.; Clough, M. T.; Ralph, J.; Kennema, M.; Bruijnincx, P. C. A.; Weckhuysen, B. M. Paving the Way for Lignin Valorisation: Recent Advances in Bioengineering, Biorefining and Catalysis. *Angew. Chem., Int. Ed.* **2016**, *55*, 8164−8215.

(6) Schutyser, W.; Renders, T.; Van den Bosch, S.; Koelewijn, S.-F.; Beckham, G. T.; Sels, B. F. Chemicals from Lignin: An Interplay of Lignocellulose Fractionation, Depolymerisation, and Upgrading. *Chem. Soc. Rev.* **2018**, *47*, 852−908.

(7) Sun, Z.; Fridrich, B.; de Santi, A.; Elangovan, S.; Barta, K. Bright Side of Lignin Depolymerization: Toward New Platform Chemicals. *Chem. Rev.* **2018**, *118*, 614−678.

(8) Cui, Y.; Goes, S. L.; Stahl, S. S. Sequential Oxidation-Depolymerization Strategies for Lignin Conversion to Low Molecular Weight Aromatic Chemicals. In *Adv. Inorg. Chem.*; Ford, P. C., van Eldik, R., Eds.; Catalysis in Biomass Conversion; Academic Press, 2021; Vol. 77, Chapter 4, pp 99−136.

(9) Liu, B.; Abu-Omar, M. M. Lignin Extraction and Valorization Using Heterogeneous Transition Metal Catalysts. In *Adv. Inorg. Chem.*; Ford, P. C., van Eldik, R., Eds.; Catalysis in Biomass Conversion; Academic Press, 2021; Vol. 77, Chapter 5, pp 137−174.

(10) Liguori, F.; Moreno-Marrodan, C.; Barbaro, P. Biomass-derived chemical substitutes for bisphenol A: Recent Advancements in Catalytic Synthesis. *Chem. Soc. Rev.* **2020**, *49*, 6329−6363.

(11) Rahimi, A.; Ulbrich, A.; Coon, J. J.; Stahl, S. S. Formic-Acid-Induced Depolymerization of Oxidized Lignin to Aromatics. *Nature* **2014**, *515*, 249−252.

(12) Luo, H.; Weeda, E. P.; Alherech, M.; Anson, C. W.; Karlen, S. D.; Cui, Y.; Foster, C. E.; Stahl, S. S. Oxidative Catalytic Fractionation of Lignocellulosic Biomass under Non-alkaline Conditions. *J. Am. Chem. Soc.* **2021**, *143*, 15462−15470.

(13) Alherech, M.; Omolabake, S.; Holland, C. M.; Klinger, G. E.; Hegg, E. L.; Stahl, S. S. From Lignin to Valuable Aromatic Chemicals: Lignin Depolymerization and Monomer Separation via Centrifugal Partition Chromatography. *ACS Cent. Sci.* **2021**, *7*, 1831−1837.

(14) The abbreviations **H**, **G**, and **S** are commonly used in the lignin literature for the three canonical monolignols, *p*-coumaryl alcohol, coniferyl alcohol, and sinapyl alcohol. For simplicity, we use the same nomenclature here for the three lignin-derived monomers obtained from oxidative depolymerization of lignin.

(15) Jose, J. P.; Joeseph, K. Advances in Polymer Composites: Macro- and Microcomposites - State of the Art, New Challenges, and Opportunities. In *Polymer Composites: Vol. I*; Thomas, S., Joseph, K., Malhotra, S. K., Goda, K., Sadasivan, S. M., Eds.; Wiley-VCH Verlag GmbH & Co.: New York, 2012; pp 1−16.

(16) Matsuda, T.; Nakamura, T.; Sasakawa, A.; Hayashi, S.; Konai, Y. *Preparation Process of Biphenyl-4,4'-Dicarboxylic Acid*. Patent US4970338A, November 13, 1990.

(17) Edling, H. E.; Liu, H.; Sun, H.; Mondschein, R. J.; Schiraldi, D. A.; Long, T. E.; Turner, S. R. Copolyesters Based on Bibenzoic acids. *Polymer* **2018**, *135*, 120−130.

(18) Asrar, J. Synthesis and Properties of 4,4'-Biphenyldicarboxylic Acid and 2,6-Naphthalenedicarboxylic Acid. *J. Polym. Sci., Part A: Polym. Chem.* **1999**, *37*, 3139−3146.

(19) Dakka, J. M.; Decaul, L. C.; Costello, C. A.; Mozeleski, E. J.; Osterrieth, P. J.; Smirnova, D. S.; Zushma, S.; Godwin, A. D.; Faler, C. A.; Deflorio, V.; Naert, D. *Alkyl Aromatic Hydroalkylation for the Production of Plasticizers*. Patent WO2014117076A9, April 23, 2015.

(20) Dakka, J. M.; DeCaul, L. C. *Methyl-Substituted Biphenyl Compounds, Their Production and Their Use in the Manufacture of Plasticizers*. Patent US9663417B2, May 30, 2017.

(21) Mazoyer, E.; Lotz, M. D.; Bokis, C. P.; Guzman, J. *Preparation and Purification of Biphenyldicarboxylic Acids*. Patent US20200361847A1, November 19, 2020.

(22) Zembayashi, M.; Tamao, K.; Yoshida, J.; Kumada, M. Nickel-Phosphine Complex-Catalyzed Homocoupling of Aryl Halides in the Presence of Zinc Powder. *Tetrahedron Lett.* **1977**, *18*, 4089−4091.

(23) Iyoda, M.; Sato, K.; Oda, M. Nickel-catalyzed Coupling of Bromides of 1,6-Methano[10]annulene and Azulene. A facile

Synthesis of Biannulene and Bi-, Ter-, Quater-, and Polyazulenes. *Tetrahedron Lett.* **1985**, *26*, 3829−3832.

(24) Qian, Q.; Zang, Z. H.; Wang, S. L.; Chen, Y.; Lin, K. H.; Gong, H. G. Nickel-Catalyzed Reductive Cross-Coupling of Aryl Halides. *Synlett* **2013**, *24*, 619−624.

(25) Liao, L. Y.; Kong, X. R.; Duan, X. F. Reductive Couplings of 2-Halopyridines without External Ligand: Phosphine-Free Nickel-Catalyzed Synthesis of Symmetrical and Unsymmetrical 2,2′-Bipyridines. *J. Org. Chem.* **2014**, *79*, 777−782.

(26) Yamashita, J.; Inoue, Y.; Kondo, T.; Hashimoto, H. Ullmann-Type Coupling Reaction of Aryl Trifluoromethanesulfonates Catalyzed by in Situ-Generated Low Valent Nickel Complexes. *Chem. Lett.* **1986**, *15*, 407−408.

(27) Jutand, A.; Mosleh, A. Palladium and Nickel Catalyzed Synthesis of Biaryls from Aryl Triflates in the Presence of Zinc Powder. *Synlett* **1993**, *1993*, 568−570.

(28) Rosen, B. M.; Quasdorf, K. W.; Wilson, D. A.; Zhang, N.; Resmerita, A.; Garg, N. K.; Percec, V. Nickel-Catalyzed Cross-Couplings Involving Carbon−Oxygen Bonds. *Chem. Rev.* **2011**, *111*, 1346−1416.

(29) Maddaluno, J.; Durandetti, M. Dimerization of Aryl Sulfonates by in Situ Generated Nickel(0). *Synlett* **2015**, *26*, 2385−2388.

(30) Rahil, R.; Sengmany, S.; Gall, E. L.; Léonel, E. Nickel-Catalyzed Electrochemical Reductive Homocouplings of Aryl and Heteroaryl Halides: A Useful Route to Symmetrical Biaryls. *Synthesis* **2018**, *50*, 146−154.

(31) Qiu, H.; Shuai, B.; Wang, Y.-Z.; Liu, D.; Chen, Y.-G.; Gao, P.-S.; Ma, H.-X.; Chen, S.; Mei, T.-S. Enantioselective Ni-Catalyzed Electrochemical Synthesis of Biaryl Atropisomers. *J. Am. Chem. Soc.* **2020**, *142*, 9872−9878.

(32) Percec, V.; Bae, J.-Y.; Zhao, M.; Hill, D. H. Aryl Mesylates in Metal-Catalyzed Homocoupling and Cross-Coupling Reactions. 1. Functional Symmetrical Biaryls from Phenols via Nickel-Catalyzed Homocoupling of Their Mesylates. *J. Org. Chem.* **1995**, *60*, 176.

(33) Jutand, A.; Mosleh, A. Nickel- and Palladium-Catalyzed Homocoupling of Aryl Triflates. Scope, Limitation, and Mechanistic Aspects. *J. Org. Chem.* **1997**, *62*, 261−274.

(34) Ackerman, L. K. G.; Lovell, M. M.; Weix, D. J. Multimetallic Catalysed Cross-Coupling of Aryl Bromides with Aryl Triflates. *Nature* **2015**, *524*, 454−457.

(35) Huang, L.; Ackerman, L. K. G.; Kang, K.; Parsons, A.; Weix, D. J. LiCl-Accelerated Multimetallic Cross-Coupling of Aryl Chlorides with Aryl Triflates. *J. Am. Chem. Soc.* **2019**, *141*, 10978−10983.

(36) Kang, K.; Loud, N. L.; DiBenedetto, T. A.; Weix, D. J. A General, Multimetallic Cross-Ullmann Biheteroaryl Synthesis from Heteroaryl Halides and Heteroaryl Triflates. *J. Am. Chem. Soc.* **2021**, *143*, 21484−21491.

(37) Kang, K.; Huang, L.; Weix, D. J. Sulfonate Versus Sulfonate: Nickel and Palladium Multimetallic Cross-Electrophile Coupling of Aryl Triflates with Aryl Tosylates. *J. Am. Chem. Soc.* **2020**, *142*, 10634−10640.

(38) Xiong, B.; Li, Y.; Wei, Y.; Kramer, S.; Lian, Z. Dual Nickel-/Palladium-Catalyzed Reductive Cross-Coupling Reactions between Two Phenol Derivatives. *Org. Lett.* **2020**, *22*, 6334−6338.

(39) Ni-only catalyst systems have been used under electrochemical conditions to support reductive biaryl cross-coupling with certain privileged substrate classes, such as the coupling of 2-halopyridine with aryl halides. See, for example, refs 40−42.

(40) Gosmini, C.; Lasry, S.; Nedelec, J.-Y.; Périchon, J. Electro-chemical Cross-Coupling between 2-Halopyridines and Aryl or Heteroaryl Halides Catalysed by Nickel-2,2′-Bipyridine Complexes. *Tetrahedron* **1998**, *54*, 1289−1298.

(41) Gosmini, C.; Nédélec, J. Y.; Périchon, J. Electrochemical Cross-Coupling between Functionalized Aryl Halides and 2-Chloropyr-imidine or 2-Chloropyrazine Catalyzed by Nickel 2,2′-Bipyridine Complex. *Tetrahedron Lett.* **2000**, *41*, 201−203.

(42) Gosmini, C.; Nédélec, J. Y.; Périchon, J. Electrosynthesis of Functionalized 2-Arylpyridines from Functionalized Aryl and Pyridine

Halides Catalyzed by Nickel Bromide 2,2′-Bipyridine Complex. *Tetrahedron Lett.* **2000**, *41*, 5039−5042.

(43) Wills, A. G.; Charvet, S.; Battilocchio, C.; Scarborough, C. C.; Wheelhouse, K. M. P.; Poole, D. L.; Carson, N.; Vantourout, J. C. High-Throughput Electrochemistry: State of the Art, Challenges, and Perspective. *Org. Process Res. Dev.* **2021**, *25*, 2587.

(44) Rein, J.; Annand, J. R.; Wismer, M. K.; Fu, J.; Siu, J. C.; Klapars, A.; Strotman, N. A.; Kalyani, D.; Lehnherr, D.; Lin, S. Unlocking the Potential of High-Throughput Experimentation for Electrochemistry with a Standardized Microscale Reactor. *ACS Cent. Sci.* **2021**, *7*, 1347−1355.

(45) Cywar, R. M.; Rorrer, N. A.; Hoyt, C. B.; Beckham, G. T.; Chen, E. Y.-X. Bio-Based Polymers with Performance-Advantaged Properties. *Nat. Rev. Mater.* **2022**, *7*, 83−103.

(46) For similar observations, see: Kawamata, Y.; Vantourout, J. C.; Hickey, D. P.; Bai, P.; Chen, L.; Hou, Q.; Qiao, W.; Barman, K.; Edwards, M. A.; Garrido-Castro, A. F.; deGruyter, J. N.; Nakamura, H.; Knouse, K.; Qin, C.; Clay, K. J.; Bao, D.; Li, C.; Starr, J. T.; Garcia-Irizarry, C.; Sach, N.; White, H. S.; Neurock, M.; Minteer, S. D.; Baran, P. S. Electrochemically Driven, Ni-Catalyzed Aryl Amination: Scope, Mechanism, and Applications. *J. Am. Chem. Soc.* **2019**, *141*, 6392−6402.

(47) Klein, P.; Lechner, V. D.; Schimmel, T.; Hintermann, L. Generation of Organozinc Reagents by Nickel Diazadiene Complex Catalyzed Zinc Insertion into Aryl Sulfonates. *Chem.—Eur. J.* **2020**, *26*, 176−180.

(48) Martin, R.; Buchwald, S. L. Palladium-Catalyzed Suzuki-Miyaura Cross-Coupling Reactions Employing Dialkylbiaryl Phosphine Ligands. *Acc. Chem. Res.* **2008**, *41*, 1461−1473.

(49) Olivares, A. M.; Weix, D. J. Multimetallic Ni- and Pd-Catalyzed Cross-Electrophile Coupling to Form Highly Substituted 1,3-Dienes. *J. Am. Chem. Soc.* **2018**, *140*, 2446−2449.

(50) Xiong, B.; Chen, X.; Liu, J.; Zhang, X.; Xia, Y.; Lian, Z. Stereoselective Gem-Difluorovinylation of Gem-Difluorinated Cyclo-propanes Enabled by Ni/Pd Cooperative Catalysis. *ACS Catal.* **2021**, *11*, 11960−11965.

(51) Martin, T. M. *T. E. S. T. (Toxicity Estimation Software Tool) Version 5.1*; United State Environmental Protection Agency, 2020.

(52) *Chemical Transformation Simulator (CTS), Version 1.0.*; United State Environmental Protection Agency, 2019.